Particle Size and Crystallinity Dependent Electron Injection in Fluorescein 27-Sensitized TiO_2 Films

Gábor Benkö,[†] Björn Skårman,[‡] Reine Wallenberg,[‡] Anders Hagfeldt,[§] Villy Sundström,[†] and Arkady P. Yartsev*,[†]

Departments of Chemical Physics and Materials Chemistry, Lund University, Box 124, SE−22100, Lund, Sweden, and Department of Physical Chemistry, Uppsala University, Box 532, SE−75121, Uppsala, Sweden

Received: July 3, 2002; In Final Form: November 8, 2002

Influence of processing parameters, such as autoclaving and firing temperature, on the optical properties of nanocrystalline anatase TiO_2 film and on the process of electron injection from the dye fluorescein 27 to the as-prepared films is studied. Transmission electron microscopy and steady-state and time-resolved femtosecond spectroscopy measurements indicate that the larger the TiO_2 particle and the better its overall crystallinity, the faster the process of electron injection. Unraveling factors that control the properties of the sub-20-nm sized semiconductor particles, and by this the electron injection to them, is important for understanding the process of interfacial electron transfer from the dye to the semiconductor, as well as future optimization of the function of the photoelectrochemical cell based on dye-sensitized TiO_2 films.

1. Introduction

At the heart of a photoelectrochemical cell (so-called Grätzel-type dye-sensitized solar cell; DSSC)[1−6] is a porous nanocrystalline semiconductor oxide film covered by a monolayer of a sensitizing dye. The role of the dye molecule in light-energy conversion is to act as an antenna. It captures the energy of sunlight, which initiates a long-lived charge-separated state when an electron from the photoexcited state of the dye is injected into the conduction band of the semiconductor. The task of the film is to host the dye molecules, and upon electron arrival guarantee the transfer of the electrons to the outer electric circuit. The successful strategy to accomplish substantial sunlight absorption, i.e., host a high number of dye molecules, is to fabricate TiO_2 films with a high internal surface area, consisting of nanoparticles (<20 nm). Such films are commonly prepared via a sol−gel procedure.[1−6] As a result of the preparation, the films have a heterogeneous structure of an interconnected network of individual particles with large particle and pore size distribution, multiple exposed crystal faces, and variation in the surface and bulk defect densities. These characteristics make the nanoparticle film one of the most puzzling components of the DSSC. The impact of heterogeneity, as a result of the preparation of the nanocrystalline film, on the electron injection process is discussed below.

The surface structure of the semiconductor particle determines the efficiency of the dye adsorption. A heterogeneous surface structure, resulting from, e.g., dislocations and abrupt termination of the crystal lattice at the surface, will lead to a variation in the interaction between the dye and semiconductor. For example, the binding of the dye to various particle surfaces results in a variety of anchoring geometries for the dye that may influence the kinetics of interfacial electron injection between the molecule and the particle.[2−5] Interfacial electron injection is an essential reaction in the DSSC because it leads to the charge-separated state, which is a critical step in the functioning of the DSSC. For example, in the most successful dye−TiO_2 film couple (Ru−polypyridine-complex-sensitized TiO_2 film)[2] electron injection proceeds on the femto- and picosecond time scales.[7]

When the particle contains defects, as a consequence of the sol−gel preparation,[1−6] the electronic and physical structures of the particle are disturbed. Having their energy levels located below the bottom of the conduction band, defects may speed up the injection and capture the electrons, as the reaction driving force (defined in terms of the classical electron transfer theory) is higher in this case. Defects can also affect the spatial overlap and electronic contact between the different nanoparticles and trap the free electrons when they are transported through the interconnected network of particles to the outer electric circuit. As a result, a significant part of the trapped electrons does not have enough time to reach the outer circuit before recombination, thus they do not perform work in the DSSC. Consequently, the crystallinity of the particles (i.e., the extent of defects) most likely influences the electron injection and further transport of electrons through the film.

Recently, the material content, chemical composition, structure, and morphology of the nanostructured TiO_2 layer were identified as important parameters controlling the overall performance of the DSSC.[2,8,9] How these preparation parameters of the TiO_2 film influence the process of electron injection from the excited state of the dye into the particle was not yet investigated. Such studies are not only of technological importance but also of basic scientific interest in describing the appropriate model for electron transfer (ET) in dye-sensitized semiconductors.

In the present study we use the dye fluorescein 27 together with TiO_2 film, because this dye−semiconductor couple was previously identified to be a suitable model system for studying interfacial ET.[10] The dye itself, as well as the dye attached to both TiO_2 colloids[11,12] and nanocrystalline thin film[10] has already

* Corresponding author. E-mail: Arkady.Yartsev@chemphys.lu.se.
[†] Chemical Physics, Lund University.
[‡] Materials Chemistry, Lund University.
[§] Uppsala University.

10.1021/jp026442+ CCC: $25.00
Published on Web 01/21/2003

TABLE 1: TiO_2 Films Sorted by the Autoclaving Temperature Used during Preparation

anatase TiO_2 films	1	2	3	4
autoclaving of the sols [12 h]	no	175 °C	200 °C	230 °C
firing of the films [30 min]	450 °C	450 °C	450 °C	450 °C
size [TEM]	4 ± 1 nm	8 ± 3 nm		14 ± 4 nm

TABLE 2: TiO_2 Films Prepared from the Same Paste and Fired at Different Temperatures

anatase TiO_2 films	4	5	6
autoclaving of the sols [12 h]	230 °C	230 °C	230 °C
firing of the films [30 min]	450 °C	300 °C	500 °C
size [TEM]		14 ± 4 nm	

been characterized by steady-state and time-resolved spectroscopies. In the case of the dye-sensitized films it was demonstrated that the stimulated emission (SE) decay of the excited fluorescein 27 molecule is caused by electron injection into the conduction band of the TiO_2, as the decay of SE is directly correlated to the formation of ET products, which are conduction-band electrons and oxidized dye molecules.[10] Although the electronic interaction between this type of xanthene dye[13] and the TiO_2 particles is strong,[10] the injection proceeds via the localized excited state of the dye and not through a charge-transfer excited state,[10−14] as recently suggested.[15−20] The kinetics of the injection are ultrafast and nonexponential, requiring at least three time constants ranging from ∼80 fs to ∼10 ps.[10,21] The multiexponential nature of electron injection is probably associated with the heterogeneous interaction between the dye and the semiconductor (see above).[5]

Here we report results of a femtosecond visible transient absorption study focusing on the size and crystallinity of the TiO_2 particles that influence the rate of electron injection in fluorescein 27-sensitized TiO_2 films. To our knowledge, this is the first reported study on a dye−TiO_2 film system where the dependence of electron injection on these parameters was monitored on the femtosecond and picosecond time scales.

2. Experimental Section

Dye-Sensitized TiO_2 Films. Preparation of porous TiO_2 films was carried out according to the well-established sol−gel procedure.[2,5,6] Briefly, stock solutions of TiO_2 colloids were prepared by controlled hydrolysis of titanium isopropoxide using 0.1 M HNO_3, followed by autoclaving for about 12 h at different temperatures leading eventually to three different colloidal solutions (pastes), 1−3; see Table 1 for details. The fourth type (4) of TiO_2 solution was prepared according to the same recipe by Solaronix SA.

To obtain films of uniform thickness of ∼1.5 μm, we have used Scotch tape as a frame and spacer, and a glass rod to spread the sols over 0.8 × 76 × 26 mm microscope glass cover slips. The films were dried in air at room temperature for about 1 h, and finally sintered at 450 °C for 30 min to burn out the organic content and obtain transparent TiO_2 films that are suitable for ultrafast spectroscopic measurements (see Table 1 for details). At the same time two replicas of film 4, numbered 5 and 6, were made and fired at 300 and 500 °C, respectively (see Table 2 for details).

It is important to mention that at the preparation of films 5 and 6 a single film has been made, which was cut into two pieces that were fired at different temperatures. For steady-state measurements, ultrathin (∼0.1 μm) versions of films 5 and 6, named 5UT and 6UT, were prepared using the colloidal solution 4. During the deposition of the ultrathin films no spacer-tape was used. The thickness of the thick films was measured by a profilometer, whereas the thickness of the ultrathin films was estimated by Beer−Lambert law.

The fluorescein 27 laser dye was used as purchased from Lambda Physik. Sensitization of the TiO_2 films was carried out by soaking the films in a 1.5×10^{-4} M solution of fluorescein 27 in CH_3CN. At the end of the sensitization procedure, the films were dried under nitrogen, rinsed with solvent, dried again, and finally covered with an 80 μm thick microscope glass cover slip. During purging of the dye-sensitized films with solvent, the optical density of the sensitized films (adjusted to ∼1.0 at the excitation wavelength) did not change, showing that all dye molecules were adsorbed to the surface. Before sealing, a drop of CH_3CN was introduced between the film and the cover glass. The samples were prepared immediately prior to measurements. To prevent degradation of the adsorbed dye due to laser light irradiation, the samples were continuously moved during measurements by using an X−Y translation stage. No degradation or modification of the samples was observed in steady-state spectra recorded before and after the pump−probe measurements. All the experiments presented in this work were repeated for several different samples prepared in the same way, and very similar results were obtained. Some of these results are presented in the Supporting Information.

Transmission Electron Microscope (TEM). The samples were investigated in a JEM 2000FX TEM. The microscope has a resolving power of ∼2.5 Å at 200 kV and is equipped with a slow-scan CCD camera for direct digital recording as well as traditional photographic film. The TiO_2 films were gently removed from the glass substrate and grinded by dipping in a methanol suspension before dispersion onto holey carbon copper grids. The average sizes of the TiO_2 particles were calculated from several TEM pictures by counting a large number of particles.

Femtosecond Spectrometer. Femtosecond pump−probe measurements were performed on a differential absorption spectrometer based on a regeneratively amplified 5 kHz repetition rate mode-locked Ti:Sapphire laser system in combination with an optical parametric amplifier. A more detailed description of this setup has been presented previously.[10]

To resolve the initial dynamics following photoexcitation of the adsorbed dye, we have used femtosecond pump−probe spectroscopy, exciting the dye with a 520 nm, ∼100 fs laser pulse. A typical excitation pulse energy of ∼0.5 μJ was used with a spot diameter of ∼400 μm at the sample position. For the generation of probe and reference light, part of the amplified fundamental laser beam was sent into a sapphire plate to generate a white-light continuum. The mutual polarization of the excitation and analyzing beams were kept at magic-angle orientation. For selecting the 570 nm detection wavelength, the probe and reference beams were dispersed in a monochromator. The spectral resolution of the detection system was 5 nm. The transient absorption signal was measured by detecting the probe, reference, and part of the excitation light with three photodiodes in a single shot detection system. Changes in absorbance as low as 10^{-5} could be recorded by this system. The instrument response function of ∼120 fs (fwhm) was determined by sum frequency cross correlation in a BBO crystal. For monitoring the dynamics following excitation of the samples, transient absorption kinetics were recorded by scanning the pump−probe delay time. The accurate zero-time delay was independently determined by sum frequency cross-correlation measurements and by the nonresonant "spike-signal" in a 1 mm thick glass plate. For very precise determination of the zero time, the low amplitude "spike-signal" ($\Delta A_{max} < 1.0 \times 10^{-4}$) generated in a

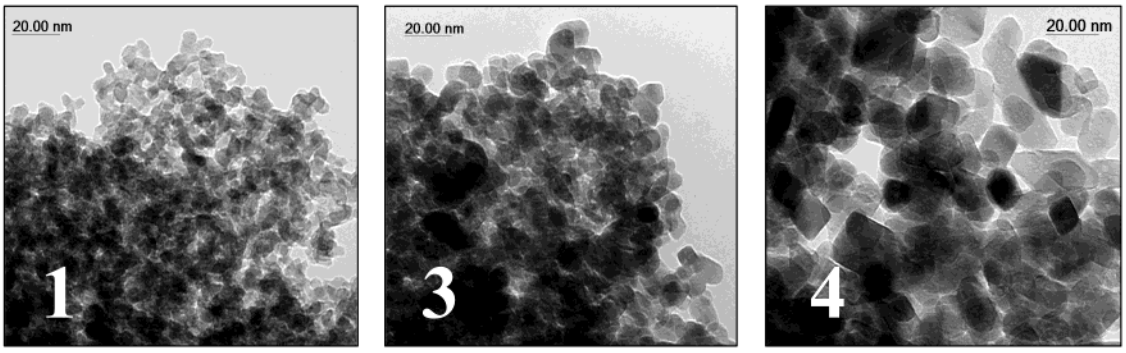

Figure 1. TEM images of films prepared from pastes autoclaved at different temperatures: (1) film 1; (3) film 3; (4) film 4. See text and Table 1 for details. The magnification is 120kX in all three images.

80 μm glass slide was recorded (such a thin glass slide was used as front window of our sample cell). See Supporting Information for results obtained on several different samples prepared in a similar way. All experiments were conducted at room temperature. Measured kinetics were analyzed with the deconvolution software Spectra Solve 2.01, LASTEK Pty. Ltd. 1997.

3. Results and Discussion

I. Characterization of Nonsensitized (Naked) and Sensitized TiO_2 Films. Before time-resolved experiments could be performed, the films had to be characterized by steady-state methods. We have used TEM, electron diffraction analysis, and steady-state absorption spectrum measurements to determine the major characteristics of the TiO_2 nanoparticle films that are relevant to the process of ET from a dye molecule to a nanoparticle.

Influence of Autoclaving Temperature. Autoclaving of the stock TiO_2 solutions allows controlled growth of the primary particles. During this hydrothermal growth the smaller particles dissolve and fuse to larger particles by the Ostwald ripening process.[2−5] Our films were autoclaved at different temperatures that do not exceed 240 °C, where rutile formation is known to start.[9] We did not observe any other crystal phases than anatase by examining electron diffraction patterns for all of the investigated samples.

Considering the films that were all prepared according to the same procedure and fired at 450 °C (films 1−4; see Table 1), we expect substantial variation in the size of the particles building up the films, resulting from the different autoclaving temperatures.[2−5,9] Indeed, as shown in the panels of Figure 1, there is a clear difference between the TEM images of the films. The average diameters of the particles in each of the films are given in Table 1. The crystallite size, size distribution, and structure of particles in films 2 and 3 were found to be very similar (8 ± 3 nm), that is why only one representative image of film 3 is shown in Figure 1. On the basis of previous studies,[2−5,9] the size of the particles in film 3 is supposed to be somewhat larger than in film 2. Because the films have a wide spread in particle size, it is difficult to detect small changes in the mean value of the particle size induced by the higher autoclaving temperature in film 3. In summary, the results show that the higher the autoclaving temperature, the larger the size of the particles. No information regarding the effect of autoclaving temperature on crystallinity of the films could be obtained from the TEM studies. Nevertheless, autoclaving temperature should also have influence on the crystal structure, pore-size distribution, crystallographic orientation of the particle faces, and aggregation of the particles,[9] but investigation of these parameters is beyond the scope of this work.

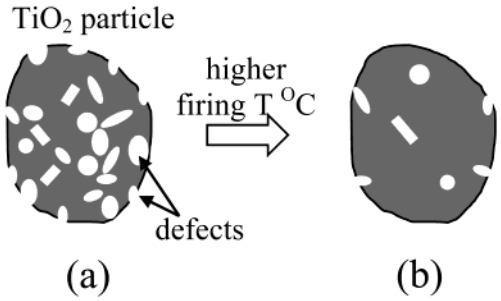

Figure 2. Changes induced by firing temperature on the TiO_2 particle. The particle with high concentration of defects (shown by white spots) (a) is transformed into a particle with low concentration of defects (b). The change in particle size and morphology on firing is expected to be small.[24]

Influence of Firing Temperature. Because the stock colloidal solutions contain organic additives, temperatures around 450 °C are usually applied for firing films of 5−10 μm thickness that are used in DSSC. During firing, the organic additives are burned out. By this, a compact spongelike network of electronically connected nanoparticles is produced.[1−6] On the basis of previous reports,[8,22−24] increasing the firing temperature within the range where the anatase single phase still exists for the TiO_2 thin films (between 250 and 600 °C) results in both an increase in particle size[22,23] as well as an increase in the overall crystallinity of each particle.[24] This latter characteristic, illustrated in Figure 2, leads to an increase in the quality of the nanoparticle surface, i.e., a decrease in the concentration of defects.[24]

We have chosen temperatures of 300 (film 5), 450 (film 4), and 500 °C (film 6) to sinter the TiO_2 films (Table 2), in an attempt to identify any variation in, e.g., particle size and structure, as suggested by previous reports,[22,23] but again, we could not observe any clear difference by TEM analysis (images not shown). As a difference in electron injection is clearly noticeable from the fluorescein 27 dye to the films 4−6 (see next section, Figure 5), we do expect to see variation in the crystallinity of the particles with firing temperature. Another way to compare the crystallinity of the TiO_2 films is to measure their linear absorption spectrum and compare the long absorption tail in the visible spectral region that is typical of TiO_2 containing defects.[5,24] It is important to point out that the recording of the linear absorption of the few micrometer thick TiO_2 films in transmission mode is difficult.[25] Their absorption in the UV is far beyond the measurement range of conventional spectrophotometers, whereas the weak absorption of defects in

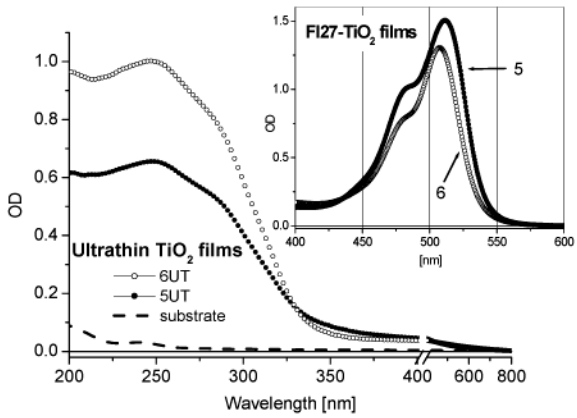

Figure 3. Steady-state absorption spectra of naked ultrathin (~0.1 μm) TiO_2 films that were fired at different temperatures (films 5UT and 6UT), and the quartz substrate (dashed line). Inset: steady-state absorption spectra of fluorescein 27-sensitized 1.5 μm thick TiO_2 films (sample 5 and 6) that were fired at different temperatures.

the visible spectral region is often hidden by thin film interference modulations (see Supporting Information).

To compare the linear absorption spectra of the TiO_2 films, we carefully recorded the spectra of films fired at different temperatures. To this end, an ultrathin (~0.1 μm) very homogeneous TiO_2 film was prepared from paste 4 on a quartz substrate and cut into two parts. Such a preparation ensures the same low concentration and quality of the starting material for both parts, which is important for the comparison of the steady-state absorption spectra (Supporting Information).[25] The two films were fired at 300 (film 5UT) and 500 °C (film 6UT), respectively.

The steady-state spectra of the naked ultrathin films 5UT and 6UT are shown in the main panel of Figure 3. Contrary to the TEM investigations, the optical measurements show clear difference between the films. The UV spectral region is dominated by the indirect and direct band transitions of the semiconductor,[25,26] whereas the absorption in the visible (between 350 and 800 nm) is due to the states below the conduction band, attributed to various defect states.[5,24,27] Because the concentration of TiO_2 (see the Experimental Section), scattering[28] or quantum size effects[25,26,29] are not responsible for the changes we observe, the large difference between the two spectra indicates that firing at higher temperature causes an increase in the crystallinity of the particles, similar to what has been observed in ref 24 (Figure 2). By firing at a higher temperature the absorption/concentration of the defects decreases, while at the same time the absorption of the band transitions increases (Figure 3). The observed changes of the different bands in the UV and visible spectral regions indicate a transition from particles with more defects to particles with less defects. Consequently, the number of basic crystal structures increases (size of the particle should increase[22−23]), leading to a higher density of acceptor states in the energy bands. The spectral changes in Figure 3 can also point toward a decrease in the amorphous material content, but no substantial amount of amorphous material was detected in any of the samples in the TEM images and electron diffraction patterns. These findings show that the optical properties of the TiO_2 films are influenced by the presence of the defects, and firing at higher temperature improves the overall crystallinity, which leads to changes in the optical properties of the films.

Changes induced on the films by different firing temperatures can also be observed when the films are sensitized. For this purpose the thicker variants (1.5 μm) of the TiO_2 films were used. The steady-state absorption spectra of fluorescein 27-sensitized films 5 and 6 are presented in the Figure 3 inset. The difference in optical density between the samples can be rationalized as follows. Due to the higher firing temperature the size of the particles and pores increases, the surface area decreases, and as a result fewer dye molecules can be adsorbed per unit volume of the film.[9,22,23] That is why the absorption of the sensitized film 6 is lower. The wavelength shift of the spectrum with firing temperature (Figure 3 inset) is most likely because the adsorption characteristic of the dye varies with the quality of the particle surfaces. When the overall concentration of defects in the particle decreases, the concentration of surface defects is also decreasing.[24] As discussed in the Introduction, the difference in the surface quality induced by temperature may lead to a change in the interaction between the dye and the particle, which results in a modification of the absorption spectrum. Other possible reasons for the modification of the dye absorption spectrum upon adsorption to the two films (5 and 6) can be eliminated. Insufficient burning of the binder as a reason for the changed absorption amplitude would result in an effect opposite what was observed. Formation of fluorescein 27 aggregates on the TiO_2 is unlikely. For example, samples of optical density 0.4 and 1.2 at maximum absorption wavelength show identical shapes of linear absorption spectra and electron injection kinetics (Supporting Information). Moreover, it has been shown that the tendency of fluorescein 27 laser dye to aggregate is very low compared to other xanthene dyes and decreases considerably in organic solvents,[30] such as CH_3CN that is used here, compared to aqueous solution. In summary, we conclude that firing not only can improve crystallinity and the optical properties of the nanocrystalline TiO_2 films, but also indirectly influences dye adsorption and absorption.

II. Particle Size and Crystallinity Dependent Electron Injection in Fluorescein 27-Sensitized TiO_2 Films. The discussion above as well as information in previous reports[2,5−9,22−24] shows that somewhat varying preparation conditions produce films with different particle sizes and crystallinities. We will now focus on the process of electron injection from the excited state of the fluorescein 27 dye to the conduction band of the TiO_2 films (Tables 1 and 2) by using femtosecond transient absorption spectroscopy.

As mentioned in the Introduction, the fluorescein 27-sensitized TiO_2 film is an advantageous model system for studying interfacial electron transfer, because the well-characterized electron injection in this system can be easily followed by recording the SE decay of the dye.[10] The kinetics of electron injection from the fluorescein 27 dye to the films 1−4 (different autoclaving temperature) and 4−6 (different firing temperature) are shown in Figures 4 and 5, respectively. The dynamics of electron injection are ultrafast and nonexponential. This is likely a result of the heterogeneous properties of the fluorescein 27-TiO_2 system that are revealed by the TEM analysis and absorption spectroscopy measurements. We have used a multiexponential global analysis to characterize the measured kinetics, requiring at least three time constants ranging from <100 fs to ~10 ps.

The parameters of the global fit performed simultaneously on the kinetics of Figure 4 are given in Table 3. They show a gradual decrease and increase, respectively, in the amplitude of the slower (1 and 10 ps) and faster (90 fs) time constants of electron injection in samples 1 through 4. In other words, there are more fluorescein 27 molecules that are able to inject faster into the TiO_2 film 4 than into 3, then 2, and 1. The fastest injection occurs in sample 4 (14 nm) where more than 50% of

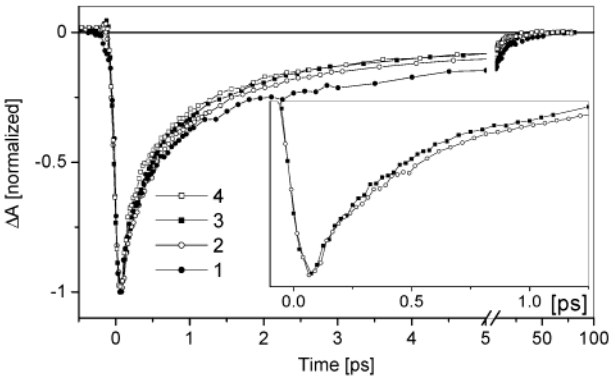

Figure 4. Electron injection kinetics at 570 nm (SE decay) in fluorescein 27-sensitized TiO_2 films with different particle sizes: the larger the anatase particles, the faster the interfacial electron injection into it. Inset: kinetics in samples 2 and 3, shown at early time delays. Fits to the measured data are not shown for clarity. The fit parameters are given in Table 3.

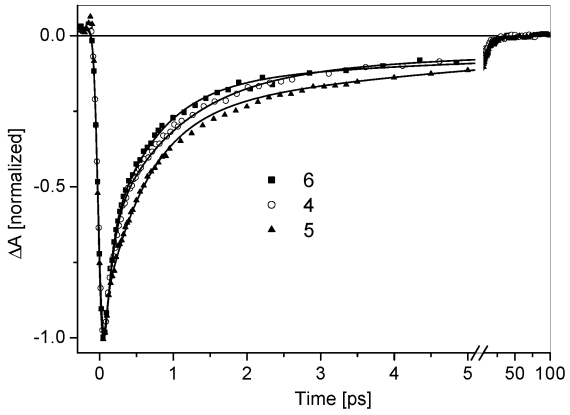

Figure 5. Electron injection kinetics at 570 nm (SE decay) in fluorescein 27-sensitized TiO_2 films of different crystallinity. The higher the crystallinity of the anatase particles, the faster the interfacial electron injection into it. Symbols are measured data, and curves are fits to the signals. The fit parameters are given in Table 4.

TABLE 3: Global Fit Parameters to Kinetics Measured at 570 nm in the Fluorescein 27-Sensitized TiO_2 Films Prepared from Pastes Autoclaved at Different Temperatures

	fit parameters (decays)			
Fl27-sensitized TiO_2 film	0.09 ps	1 ps	10 ps	const
4	54%	38%	7%	1%
3	47%	43%	9%	1%
2	43%	45%	11%	1%
1	35%	46%	18%	1%

the molecules inject on the <100 fs time scale, as compared to only 35% in sample 1 (4 nm). This means that the larger the particle the faster the electron injection from the dye to the semiconductor. Besides crystallinity, the crystallographic orientation of the particle faces can lead to different interaction between the molecule and particle. Because we do not have experimental means to determine the crystallographic orientation of particle faces, we cannot distinguish whether the increase in electron injection rate in the case of the larger particles is because of the better crystallinity or variation in crystallographic orientation.

For films fired at different temperatures, we observe a clear correlation between the electron injection rate and crystallinity. The parameters of the global fit performed simultaneously on the kinetics of Figure 5 are given in Table 4. They show a gradual decrease and increase, respectively, in the amplitude

TABLE 4: Global Fit Parameters to Kinetics Measured at 570 nm in the Fluorescein 27-Sensitized TiO_2 Films Fired at Different Temperatures

	fit parameters (decays)			
Fl27-sensitized TiO_2 film	0.09 ps	1 ps	10 ps	const
6	58%	33%	8%	1%
4	54%	38%	7%	1%
5	38%	47%	14%	1%

of the slower (1 and 10 ps) and faster (90 fs) time constants of electron injection in the dye-sensitized TiO_2 films fired at 300, 450, and 500 °C. In other words, the better the overall crystallinity of the particle, the better the dye-semiconductor interaction, the faster the electron injection from the dye to the semiconductor. The fastest injection occurs to film 6, which contains the largest anatase TiO_2 particles with the highest crystallinity.

Another important aspect of this study is the influence of defects on the rate of electron injection, from the viewpoint of the electronic structure of the particles taking into account the predictions of the classical electron transfer theory implemented on these systems[27,31] (see the Introduction). The presence of the defects modifies the apparent band-gap and produces tailing on the absorption edge to longer wavelengths in the steady-state absorption of the semiconductor (Figure 3). As a consequence, the potential energy difference between the excited state of the dye and the apparent conduction-band edge ("driving force") is increased, which according to the classical electron transfer theory should speed up the injection,[27,31] resulting in faster injection in sample 5 than in sample 6. The observed dynamics of electron injection in these two samples (Figure 5), and in other dye-sensitized TiO_2 films,[32] are not consistent with the prediction. They show that the driving force of the defects have negligible, if any, direct influence on the injection rate. Rather, the increase of the conduction band density of states in the particles of larger size and favorable anchoring geometry of the dye on the surface of higher crystallinity particles leads to faster electron injection, which is in good agreement with recent calculations.[33]

4. Conclusions

We conducted a systematic study on several anatase TiO_2 films differing by only the hydrothermal growth/autoclaving temperature of the colloidal solutions and the firing temperature in the procedure of film preparation. Steady-state UV−vis absorption spectroscopy and TEM of the naked films reveal that the variation in preparation influences the size and crystallinity (concentration of defects) of the TiO_2 nanoparticles. A steady-state absorption method that is sensitive to the relative concentration of defects in the porous nanoparticle TiO_2 films was presented.

The crystallinity of the semiconductor particles influences the optical properties of the film and, consequently, the interaction between the excited state of the adsorbed dye molecule and the conduction band of TiO_2. The rate of electron injection from the photoexcited fluorescein 27 xanthene dye into the TiO_2 particles increases with the particle size and overall crystallinity. We also found that the increasing potential energy difference between the excited state of the dye and the conduction band of the semiconductor, i.e., driving force, as a consequence of defects in the nanosized TiO_2 appears not to have a strong influence on electron injection.

Acknowledgment. We thank Prof. Sten-Eric Lindquist at Uppsala University and Dr. Marcus Hilgendorff for helpful

discussions. We also thank Eva Magnusson at Uppsala University and Dr. Toby Meyer at Solaronix SA for help with some of the samples. This research was funded by grants from the Delegationen för Energiförsörjning i Sydsverige (DESS), the Swedish Research Council, the Knut and Alice Wallenberg Foundation, the Crafoord Foundation, and the Trygger Foundation.

Supporting Information Available: Steady-state absorption spectra of TiO_2 films measured in transmission mode. This material is available free of charge via the Internet at http://pubs.acs.org.

References and Notes

(1) O'Regan, B.; Grätzel, M. *Nature* **1991**, *353*, 737−739.
(2) Kalyanasundaram, K.; Grätzel, M. *Coord. Chem. Rev.* **1998**, *77*, 347−414.
(3) Hagfeldt, A.; Grätzel, M. *Acc. Chem. Res.* **2000**, *33*, 269−277.
(4) Grätzel, M. *Nature* **2001**, *414*, 338−344.
(5) Grätzel, M.; Moser, J.-E. Solar Energy Conversion. In *Electron Transfer in Chemistry*; Balzani, V., Gould, I., Eds.; Wiley-VCH: Weinheim, 2001; Vol. V, pp 589−644.
(6) Grätzel, M. *J. Sol-Gel Sci. Technol.* **2001**, *22*, 7−13.
(7) Benkö, G.; Kallioinen, J.; Korppi-Tommola, J. E.; Yartsev, A. P.; Sundström, V. *J. Am. Chem. Soc.* **2002**, *124*, 489−493 and references therein.
(8) Zaban, A.; Aruna, S. T.; Tirosh, S.; Gregg, B. A.; Mastai, Y. *J. Phys. Chem. B* **2000**, *104*, 4130−4133.
(9) Barbé, C. J.; Arendse, F.; Comte, P.; Jirousek, M.; Lenzmann, F.; Shklover, V.; Grätzel, M. *J. Am. Ceram. Soc.* **1997**, *80*, 3157−3171.
(10) Benkö, G.; Hilgendorff, M.; Yartsev, A. P.; Sundström, V. *J. Phys. Chem. B* **2001**, *105*, 967−974.
(11) Hilgendorff, M.; Sundström, V. *Chem. Physics Lett.* **1998**, *287*, 709−713.
(12) Hilgendorff, M.; Sundström, V. *J. Phys. Chem. B* **1998**, *102*, 10505−10514.
(13) Two xanthene dyes, fluorescein 27 and Disodium fluorescein (Uranin), were investigated in our laboratory.
(14) Walters, K. A.; Gaal, D. A.; Hupp, J. T. *J. Phys. Chem. B* **2002**, *106*, 5139−5142.
(15) Ramakrishna, G.; Ghosh, H. N. *J. Phys. Chem. B* **2001**, *105*, 7000−7008.
(16) In ref 15, the pH of the dye-sensitized TiO_2 and ZrO_2 colloidal solutions was chosen to be 2.8. At this pH the dye is in predominantly neutral form; see ref 12 and references therein. In lack of optimum pH for chemisorption the concentration of the nonadsorbed dye is significant. The absorption of the different ionic forms of the dye contribute to the steady-state absorption spectrum rather than a charge-transfer absorption band did appear.
(17) Moser, J.; Grätzel, M.; Sharma, D. K.; Serpone, N. *Helv. Chim. Acta* **1985**, *68*, 1686−1690.
(18) In case of a xanthene dye (especially fluorescein)−TiO_2 system, direct excitation into the conduction band is not likely. It was shown that the overall electron injection from several xanthene dyes to TiO_2 is not instantaneous[10−13,17] and proceeds on the femtosecond and picosecond time scales. The authors of ref 15 do not have the time resolution to observe direct injection in the investigated systems; neither do they have any other proof to claim that this process occurs. The observed positive feature (above 550 nm)[15] is most likely originating not only from the absorption of the electrons injected in the conduction band. Their absorption yields a much smaller transient signal in the spectral region in question; the authors of ref 15 do not compare the extinction coefficient of the absorbing species with the values given in the literature.[10,19,20]
(19) (a) Rothenberger, G.; Fitzmaurice, D.; Grätzel, M. *J. Phys. Chem.* **1992**, *96*, 5983−5986. (b) Boschloo, G.; Fitzmaurice, D. *J. Phys. Chem. B* **1999**, *103*, 7860−7868. (c) van't Spijker, H.; O'Regan, B.; Goossens, A. *J. Phys. Chem. B* **2001**, *105*, 7220−7226.
(20) Kallioinen, J.; Benkö, G.; Sundstrom, V.; Korppi-Tommola, J. E. I.; Yartsev, A. P. *J. Phys. Chem. B* **2002**, *106*, 4396−4404.
(21) Recent experiments performed with higher time resolution (∼25 fs laser pulses) show that the fastest component of the electron injection in the fluorescein 27−TiO_2 system is ∼80 fs.
(22) Li, G. H.; Yang, L.; Jin, Y. X.; Zhang, L. D. *Thin Solid Films* **2000**, *368*, 163−167.
(23) Reddy, K. M.; Reddy, C. V. G.; Manorama, S. V. *J. Solid State Chem.* **2001**, *158*, 180−186.
(24) Hanley, T. L.; Luca, V.; Pickering, I.; Howe, R. F. *J. Phys. Chem. B* **2002**, *106*, 1153.
(25) Serpone, N.; Lawless, D.; Khairutdinov, R. *J. Phys. Chem.* **1995**, *99*, 16646−16654.
(26) Monticone, S.; Tufeu, R.; Kanaev, A. V.; Scolan, E.; Sanchez, C. *Appl. Surf. Sci.* **2000**, *162*, 565−570.
(27) Tachibana, Y.; Haque, S. A.; Mercer, I. P.; Moser, J. E.; Klug, D. R.; Durrant, J. R. *J. Phys. Chem. B* **2001**, *105*, 7424−7431 and references therein.
(28) No part of the curves in Figure 3, and not the difference between the two spectra, can be fitted to the scattering law.
(29) There is no size quantitization in the size regime $2R > 1.5$ nm for TiO_2 particles.[25,26]
(30) Valdes-Aguilera, O.; Neckers, D. C. *Acc. Chem. Res.* **1989**, *22*, 171−177 and references therein.
(31) See a recent review paper: Asbury, J. B.; Hao, E.; Wang, Y.; Ghosh, H. H.; Lian, T. *J. Phys. Chem. B* **2001**, *105*, 4545−4557 and references therein.
(32) Electron injection from the transition metal complex RuN_3 to TiO_2 particle films[7,20] with higher concentration of defects is slower: Benkö et al. Unpublished result.
(33) Stier, W.; Prezhdo, O. V. *J. Phys. Chem. B* **2002**, *106*, 8047−8054.